



Three-Dimensional Model of Sub-Plasmalemmal Ca^{2+} Microdomains Evoked by T Cell Receptor/CD3 Complex Stimulation

Diana Gil¹, Björn-Philipp Diercks¹, Andreas H. Guse¹ and Geneviève Dupont^{2*}

¹The Calcium Signalling Group, Department of Biochemistry and Molecular Cell Biology, University Medical Center Hamburg-Eppendorf, Hamburg, Germany, ²Unit of Theoretical Chronobiology, Faculté des Sciences CP231, Université Libre de Bruxelles (ULB), Brussels, Belgium

OPEN ACCESS

Edited by:

Ernesto Perez-Rueda,
Universidad Nacional Autónoma de
México, Mexico

Reviewed by:

Alexandre Lewalle,
King's College London,
United Kingdom
Thomas John Brett,
Washington University in St. Louis,
United States

*Correspondence:

Geneviève Dupont
Genevieve.Dupont@ulb.be

Specialty section:

This article was submitted to
Biological Modeling and Simulation,
a section of the journal
Frontiers in Molecular Biosciences

Received: 08 November 2021

Accepted: 24 January 2022

Published: 23 February 2022

Citation:

Gil D, Diercks B-P, Guse AH and
Dupont G (2022) Three-Dimensional
Model of Sub-Plasmalemmal Ca^{2+}
Microdomains Evoked by T Cell
Receptor/CD3 Complex Stimulation.
Front. Mol. Biosci. 9:811145.
doi: 10.3389/fmolb.2022.811145

Ca^{2+} signalling plays an essential role in T cell activation, which is a key step to start an adaptive immune response. During the transition from a quiescent to a fully activated state, Ca^{2+} microdomains of reduced spatial and temporal extents develop in the junctions between the plasma membrane and the endoplasmic reticulum (ER). These microdomains rely on Ca^{2+} entry from the extracellular medium, via the ORAI1/STIM1/STIM2 system that mediates store operated Ca^{2+} entry. The mechanism leading to local store depletion and subsequent Ca^{2+} entry depends on the activation state of the cells. The initial, smaller microdomains are triggered by D-myo-inositol 1,4,5-trisphosphate (IP_3) signalling in response to T cell adhesion. T cell receptor (TCR)/CD3 stimulation then initiates nicotinic acid adenine dinucleotide phosphate signalling, which activates ryanodine receptors (RyR). We have recently developed a mathematical model to elucidate the spatiotemporal Ca^{2+} dynamics of the microdomains triggered by IP_3 signalling in response to T cell adhesion (Gil et al., 2021). This reaction-diffusion model describes the evolution of the cytosolic and endoplasmic reticulum Ca^{2+} concentrations in a three-dimensional ER-PM junction and was solved using COMSOL Multiphysics. Modelling predicted that adhesion-dependent microdomains result from the concerted activity of IP_3 receptors and pre-formed ORAI1-STIM2 complexes. In the present study, we extend this model to include the role of RyRs rapidly after TCR/CD3 stimulation. The involvement of STIM1, which has a lower K_D for Ca^{2+} than STIM2, is also considered. Detailed 3D spatio-temporal simulations show that these Ca^{2+} microdomains rely on the concerted opening of ~7 RyRs that are simultaneously active in response to the increase in NAADP induced by T cell stimulation. Opening of these RyRs provoke a local depletion of ER Ca^{2+} that triggers Ca^{2+} flux through the ORAI1 channels. Simulations predict that RyRs are most probably located around the junction and that the increase in junctional Ca^{2+} concentration results from the combination between diffusion of Ca^{2+} released through the RyRs and Ca^{2+} entry through ORAI1 in the junction. The computational model moreover provides a tool allowing to investigate how Ca^{2+} microdomains occur, extend and interact in various states of T cell activation.

Keywords: T cells, ER-PM junctions, ryanodine receptors, NAADP, COMSOL, computational model, store operated calcium entry, Ca^{2+} signalling

INTRODUCTION

Calcium signaling plays a crucial role in the activation of T cells and the adaptive immune response. In particular, it controls transcriptional activation, proliferation, differentiation or secretion of cytokines (Feske, 2007; Trebak & Kinet, 2019). Increases of the free cytosolic Ca²⁺ concentration rely on Ca²⁺ release from the endoplasmic reticulum (ER) and on Ca²⁺ entry from the extracellular medium. Mobilization of internal Ca²⁺ follows the increase in *D-myo*-inositol 1,4,5-trisphosphate (IP₃) and in nicotinic acid adenine dinucleotide phosphate (NAADP), via IP₃ receptors (IP₃R) and type 1 ryanodine receptor (RYR1), respectively (Streb et al., 1983; Wolf et al., 2015). Ca²⁺ entry relies on the ORAI/STIM system that allows Ca²⁺ entry in the cytosol, at a rate that is regulated by the concentration of Ca²⁺ in lumen of the ER (Putney, 2009). When Ca²⁺ dissociates from the Ca²⁺ sensors stromal interaction molecules 1 (STIM1) and 2 (STIM2) located in the ER membrane, STIM molecules aggregate and move to so-called “junctional spaces”. These regions correspond to the narrow cytosolic spaces between the ER and PM membranes, at locations where these membranes are separated by distances smaller than 20 nm. There, STIM molecules can recruit ORAI1 to form Ca²⁺ channels allowing Ca²⁺ to enter into the cytoplasm. This process is known as capacitative or store operated Ca²⁺ entry (SOCE). The relation between SOCE and ER Ca²⁺ concentration is nonlinear, with a K_D for half activation of the order of 200 μM when it depends on the dissociation of Ca²⁺ from STIM1 and of 400 μM when it depends on the dissociation of Ca²⁺ from STIM2 (Stathopoulos et al., 2006; Brandman et al., 2007; Luik et al., 2008).

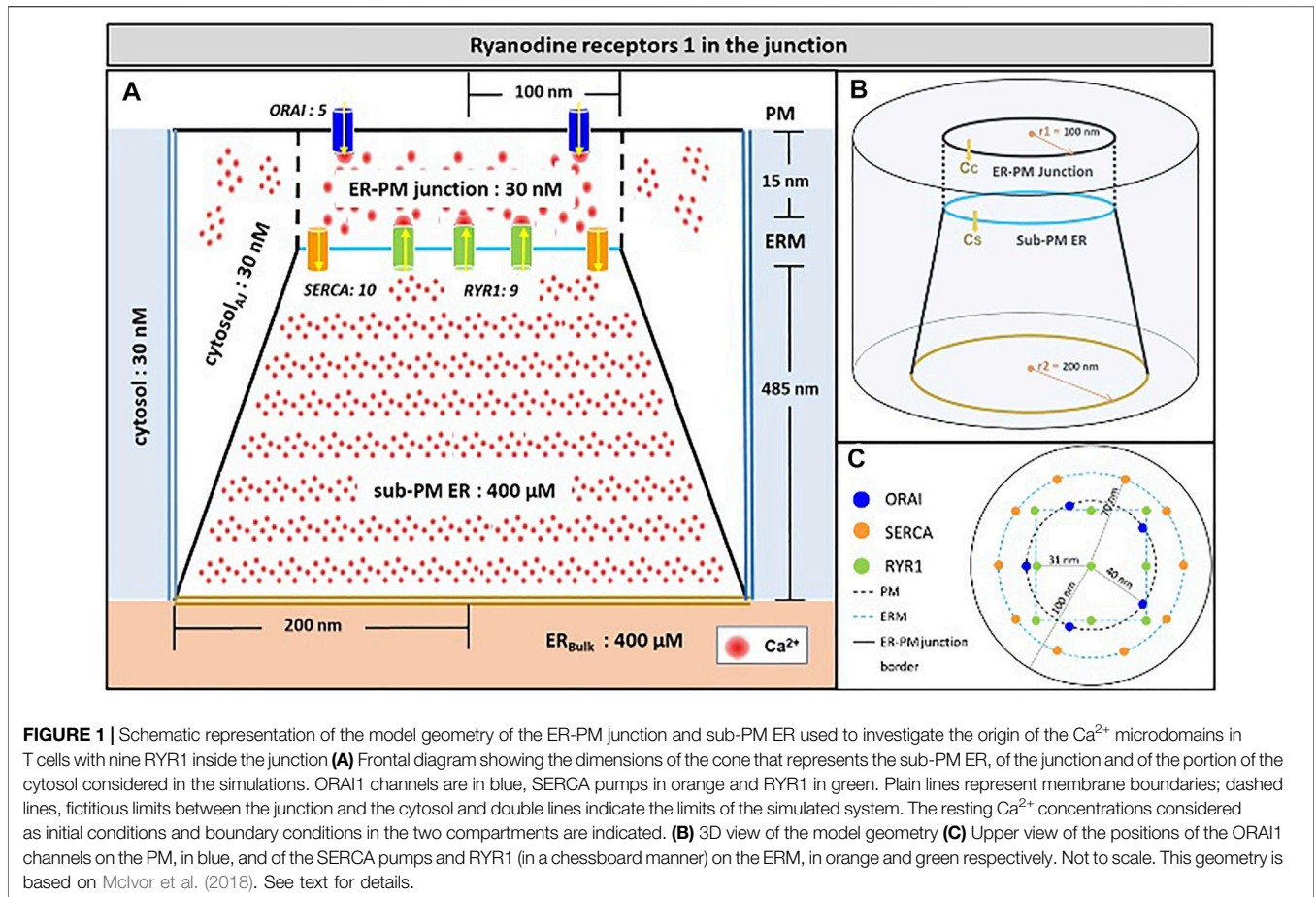
Upon TCR/CD3 stimulation, second messengers create a substantial release of Ca²⁺ from the ER which, together with the resulting activation of SOCE, leads to a rise in the free cytosolic Ca²⁺ concentration in the whole T cell. This global Ca²⁺ increase contrasts with the locally restricted, sub-plasmalemmal Ca²⁺ increases of short duration (~50 ms) that can be observed as a consequence of adhesive interactions (Weiss and Diercks, unpublished results), or in the first seconds following TCR/CD3 stimulation (Wolf et al., 2015; Diercks et al., 2018). The two types of events are known as Ca²⁺ microdomains and have similar spatio-temporal characteristics. Yet, they have different molecular origins. The adhesion dependent Ca²⁺ microdomains rely on a pathway involving focal adhesion kinase (FAK), phospholipase C (PLC) and IP₃Rs (Weiss and Diercks, unpublished results). Due to IP₃R-mediated Ca²⁺ release and subsequent SOCE, they also rely on ORAI1-mediated Ca²⁺ entry. Computational simulations of the interplay between ORAI1 and IP₃R in a 3D configuration simulating an ER-PM junction have confirmed that the local depletion of ER Ca²⁺ created by the opening of a few IP₃R can trigger the opening of ORAI1 in the junction, even in conditions of a full ER (Gil et al., 2021). Interestingly, these non-TCR/CD3 dependent Ca²⁺ microdomains require the existence of pre-formed complexes of ORAI1 and STIM2 that were demonstrated experimentally (Diercks et al., 2018). Ca²⁺ microdomains characterized by somewhat larger amplitude (340 ± 11 nM vs 290 ± 12 nM) are observed during the first

~15 s following TCR/CD3 stimulation (Wolf et al., 2015; Diercks et al., 2018; reviewed in Guse et al., 2021). As the non-TCR/CD3 dependent microdomains, these signals also involve ORAI1, but in addition they require NAADP signaling and RYR1 dependent Ca²⁺ release from ER (Wolf et al., 2015; Diercks et al., 2018). As another difference, at this stage, pre-formed ORAI1/STIM complexes involve both STIM1 and STIM2 isoforms (Ahmad et al., 2021).

Ca²⁺ microdomains represent a crucial step for the successful activation of T cells. Reported durations of the signals triggered by cell adhesion and by formation of NAADP in the first seconds upon TCR/CD3 stimulation are 44 ± 4 ms and 64 ± 3 ms, respectively (Diercks et al., 2018). They extend on 0.216 ± 0.004 μm². Because of these limited temporal and spatial extents, the investigation of Ca²⁺ microdomains is technically limited by the resolution of the microscopic imaging system used. The spatial and temporal resolution of the imaging system used to characterize T cell Ca²⁺ microdomains is approx. 368 nm and 20–25 ms, respectively (Wolf et al., 2015). Mathematical modelling thus represents a useful complementary tool to investigate their molecular origin, in the line of the numerous studies devoted to small scale Ca²⁺ events (Solovey et al., 2008; Swaminathan et al., 2009; Thul et al., 2009; Rückl & Rüdiger, 2016; Walker et al., 2017).

In a previous study (Gil et al., 2021), we adapted the realistic three-dimensional mathematical description of the ER-PM junction proposed by McIvor et al. (2018) to simulate adhesion-dependent Ca²⁺ microdomains arising in T cells. This model describes Ca²⁺ dynamics in a confined 3D configuration corresponding to a junctional cytosolic space and the adjacent sub-PM ER, taking into account Ca²⁺ influx through ORAI1 and IP₃R, Ca²⁺ pumping into the ER through SERCA, and diffusion within the cytosolic and ER compartment. The IP₃Rs are supposed to be located close to the junctional space (Thillaiappan et al., 2017). Simulations using COMSOL Multiphysics showed that the spontaneous activity of ~3 IP₃Rs create a local depletion of ER Ca²⁺ that suffices to trigger the opening of ORAI1 channels located in the junction and thus, the onset of a microdomain. Because of the presence of pre-formed complexes of ORAI1 and STIM2 in unstimulated cells, opening of ORAI1 indeed rapidly follows the dissociation of Ca²⁺ from STIM2. Predictions of this model are in agreement with recent observations in HEK293 cells reporting that constitutive STIM2 clusters in ER-PM junctions sense decreases in local ER Ca²⁺ mediated by IP₃Rs (Ahmad et al., 2021). Moreover, IP₃R channel activity near the junctions was shown to favour STIM2 clustering in the junction.

In this study, we modified our previous model of the T cell junctions to address the molecular mechanism that underlies the TCR/CD3-evoked and NAADP and RYR-dependent Ca²⁺ microdomains occurring in the first ~15 s that follow TCR/CD3 stimulation. We first used modeling to find out whether RYR1 are located inside or around the ER-PM junctions. The analysis was based on comparisons between simulated and experimental results both in WT and ORAI1^{-/-} T cells. The next issue related to the number of RYR1 involved in the formation of the junctional Ca²⁺ microdomains, which cannot



be directly inferred from experimental observations. By contrast, modeling can determine the number of RYR1 that must open simultaneously to create the local depletion of ER Ca²⁺ triggering the appropriate level of SOCE activation. Conclusions about this number were next validated by an independent estimation of the increase in the RYR1 open probability triggered by the NAADP formation in TCR/CD3 stimulated T cells. Finally, we took advantage of the great flexibility provided by computational modeling to investigate the respective roles played by the ER Ca²⁺ channels (IP₃R or RYR) and the Ca²⁺ sensors (STIM1 and STIM2) in shaping the characteristics of the Ca²⁺ microdomains created by the openings of the related ORAI1 channels. This analysis allowed us to propose a unifying description of the molecular mechanism underlying T cells Ca²⁺ microdomains from adhesion to early TCR/CD3 stimulation.

Description of the Mathematical Model

Because the model was fully described in Gil et al. (2020), we provide a concise description of its main features in this section. The spatial geometry is shown in **Figure 1**. The junction is a 15 nm-wide (Wu et al., 2006; Hogan, 2015) three-dimensional space between the PM and an ER portion located close to it. The junction communicates with the adjacent cytoplasm, a portion of which is modelled explicitly. The free cytosolic Ca²⁺ concentration, defined by C_C, is initially set at 30 nM (Diercks

et al., 2018). In the rest of the cytoplasm, which is not modelled explicitly, C_C is fixed at this same value. Similarly, the evolution of ER Ca²⁺ concentration (C_S) is simulated in the sub-PM ER, which is in contact with the bulk of the ER where Ca²⁺ concentration is fixed at 400 μM (Lewis, 2011). The PM portion located in the junction contains five ORAI channels and the ER membrane, 10 SERCA and nine RYR1s as reported (Hogan, 2015; McIvor et al., 2018; Jayasinghe et al., 2018; Yin et al., 2008). Seen from above (**Figure 1C**), SERCA pumps form a ring surrounding ORAI1 channels and RYR1s are arranged on a square lattice. Given the large size of these channels (Lanner et al., 2010), the 31 nm distance between the pores of the channels considered in **Figure 1** corresponds to a close packing of RYR1.

Membranes, schematized as simple full lines in **Figure 1A**, correspond to no flux boundary conditions, except across channels and pumps where corresponding fluxes are simulated. The flux through ORAI channels is given by

$$J_{ORAI} = f(C_S^{loc}) \frac{I_{ORAI}}{F \cdot z \cdot A_o} \tag{1}$$

with I_{ORAI} the maximal single channel current, F the Faraday constant, z the charge of a Ca²⁺ ion and A_o the surface of the channel pore. f(C_S^{loc}) is a function of the average local concentration of ER Ca²⁺ around the pore of the closest RYR1s. This step-wise function determines the level of ORAI1

activation that can take four values depending on the amount of bound Ca²⁺-free STIM. In the first phase after TCR/CD3 stimulation of T lymphocytes, preformed complexes of ORAI1, STIM1 and STIM2 have been detected by FRET experiments and super-resolution microscopy (Weiss and Diercks, unpublished results). We thus consider the activation of ORAI1 by heterotetramers of STIM1 and STIM2 (STIM1/2) and modified $f(C_S^{loc})$ accordingly. See **Supplementary Information** for a detailed explanation.

In the ER membrane, Ca²⁺ flux from the ER to the cytosol through the RYR is given by

$$J_{RYR} = \frac{I_{RYR}}{F \cdot z \cdot A_{RYR}} \cdot \frac{(C_s - C_c)}{(C_{s,0} - C_{c,0})} \quad (2)$$

with I_{RYR} the current through the RYR, which takes the value of 0.35 pA (Guo et al., 2012). A_{RYR} is the surface of the channel pore. The second factor in Eq. (2) allows to scale the current to take the actual gradient across the channel pore into account, where $C_{s,0}$ and $C_{c,0}$ represent resting concentrations of Ca²⁺ in the ER and in the cytosol (Mazel et al., 2009).

Finally, SERCA pumps are considered as bidirectional as in McIvor et al. (2018) and described by

$$J_{SERCA} = \frac{Q}{A_s} * V_{max} * \left[\frac{\left(\frac{C_c}{K_F}\right)^{n2} - \left(\frac{C_s}{K_R}\right)^{n2}}{1 + \left(\frac{C_c}{K_F}\right)^{n2} + \left(\frac{C_s}{K_R}\right)^{n2}} \right] \quad (3)$$

with V_{max} its maximal velocity, $n2$ the Hill coefficient and K_F and K_R the pump affinity for cytosolic (C_C) and ER (C_S) calcium, respectively. A_s is the surface of the pore and Q is a temperature coefficient initially introduced by McIvor et al. (2018). To approximate the partial differential equations (PDE), we used the finite element method (FEM) and simulation software COMSOL Multiphysics 5.5 (<http://www.comsol.com>), more specifically the Transport of Diluted Species interface that is used to compute the concentration field of a dilute solute in a solvent. We chose a backward differentiation formula (BDF) to compute the time steps with a relative tolerance of 0.005 that controls the relative error in each step. The system is solved using the iterative linear solver GMRES (Generalized Minimum Residual). For further details regarding the system discretization and the use of COMSOL Multiphysics, please refer to the authors.

RESULTS

Ca²⁺ Microdomains Simulated by the Opening of Type 1 Ryanodine Receptors Localized in the ER-PM Junction do Not Rely on ORAI1 Opening

Upon TCR/CD3 stimulation, NAADP-evoked Ca²⁺ release through RYR1 acts in concert with Ca²⁺ entry through ORAI1/STIM complexes to create Ca²⁺ microdomains. These microdomains last for 64 ± 3 ms and reach amplitudes of 340 ± 11 nM (Diercks et al., 2018). Although it is known that ORAI1 and STIM are arranged in pre-formed

complexes in the ER-PM junctions of T cells, the exact location of the RYR1s responsible for the decrease in $[Ca^{2+}]_{ER}$ in the sub-PM ER remains to be determined. As described in the presentation of the model and schematized in **Figure 1**, in the model we first considered that RYR1s are located in the junction, facing the PM as in cardiac dyadic clefts (Jones et al., 2018). In this section, we evaluated if this arrangement allows to reproduce experimental observations.

We simulated the junction schematized in **Figure 1** considering an increasing number of open RYR1s during 64 ms. A few milliseconds after RYR1 opening, a stable profile of Ca²⁺ increase in the junction is observed (**Figures 2A–F**, **Supplementary Figure S2**). Although C_c can locally reach concentrations close to 20 μM, the average Ca²⁺ concentration in the junction ranges from 340 to 2,500 nM depending on the number of open RYR1 (Anim. S1a,b in the **Supplementary Information**). Thus, in this configuration, opening of a single RYR1 allows to reach the experimentally observed microdomain amplitude in the junction. To assess the relative contributions of Ca²⁺ entry through ORAI1 and Ca²⁺ release from the ER through RYR1, we performed the same simulations in the absence of ORAI1 in the PM. As visible in **Figure 2H** in which Ca²⁺ microdomains with and without activated ORAI1 are seen to have nearly the same amplitude, the relative contribution of Ca²⁺ entry is very limited in these conditions. In agreement with this observation, the increase in the amplitude of the Ca²⁺ signal in the microdomain is not related to significant changes in the opening states of ORAI1 (**Figure 2I**). For example, when three RYR1s open simultaneously, all five ORAI1 channels are still in their lower state of activity as in the absence of any RYR1 opening. These computational observations indicate that the geometry depicted in **Figure 1** does not reflect the situation encountered in T-lymphocytes early after TCR activation, since the number of microdomains decreases significantly in ORAI1^{-/-} T cells (Diercks et al., 2018).

Ca²⁺ Microdomains Observed Soon After T Cell Stimulation Are due to the Opening of Type 1 Ryanodine Receptors Localized on Conic ER Around the ER-PM Junction

Because of the small size of the junction, actual Ca²⁺ concentrations are expected to be highly sensitive to the ER-PM distance. Thus, results obtained in the previous section may depend on this junctional depth, which led us to investigate the influence of this distance on the Ca²⁺ profile in the junction. Data indicate that the ER-PM spacing is typically 10–20 nm (Hogan, 2015), but we investigated distances up to 50 nm that might be reached locally. As visible in **Figure 3**, although the amplitude of the Ca²⁺ microdomain is inversely proportional to the height of the junction, the experimental average is reached with less than three RYR1 simultaneously open even for the largest junction considered (50 nm). Moreover, the amplitudes are not much affected by the absence of ORAI1, as visible by the fact that the Ca²⁺ microdomain amplitudes without ORAI1 (dashed lines) are close to those with ORAI1 (plain lines). This does not agree with experimental observations showing that in cells that do not

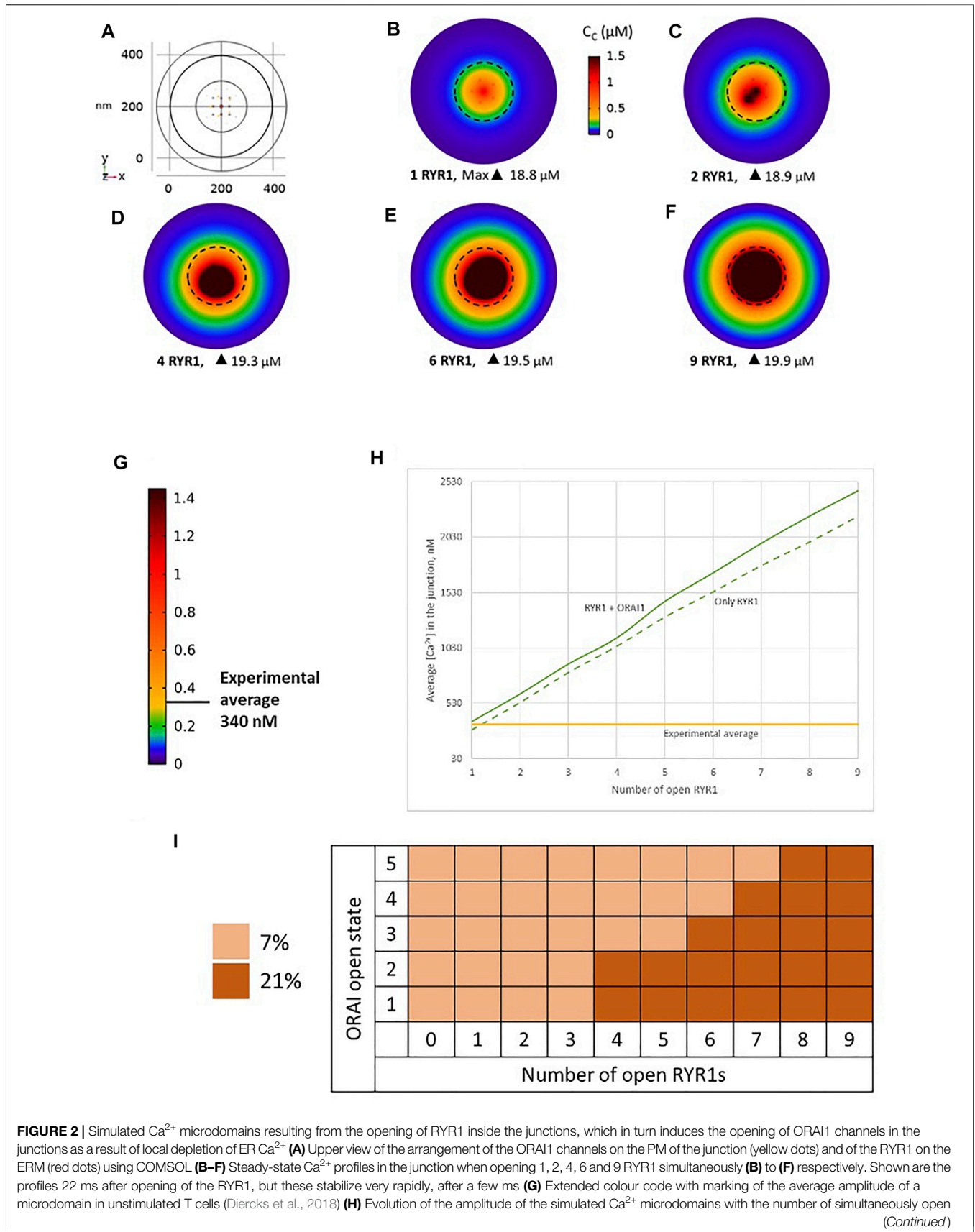


FIGURE 2 | Simulated Ca²⁺ microdomains resulting from the opening of RYR1 inside the junctions, which in turn induces the opening of ORAI1 channels in the junctions as a result of local depletion of ER Ca²⁺ (**A**) Upper view of the arrangement of the ORAI1 channels on the PM of the junction (yellow dots) and of the RYR1 on the ERM (red dots) using COMSOL (**B–F**) Steady-state Ca²⁺ profiles in the junction when opening 1, 2, 4, 6 and 9 RYR1 simultaneously (**B**) to (**F**) respectively. Shown are the profiles 22 ms after opening of the RYR1, but these stabilize very rapidly, after a few ms (**G**) Extended colour code with marking of the average amplitude of a microdomain in unstimulated T cells (Diercks et al., 2018) (**H**) Evolution of the amplitude of the simulated Ca²⁺ microdomains with the number of simultaneously open RYR1s (Continued)

FIGURE 2 | RYR1 in the junction, showing that experimentally observed microdomains do not agree with the opening of the RYRs inside the junction given the low contribution of the opening of the ORAI1 in conditions of a full ER (see text). Dotted line represents junctional Ca^{2+} concentration reached in the absence of ORAI1 channels **(I)** Individual evolution of 1–5 ORAI1 channels open state (Li et al., 2011) as a result of 0–9 RYR1 opening simultaneously. See **Supplementary Information** and Anim. S1a,b for details.

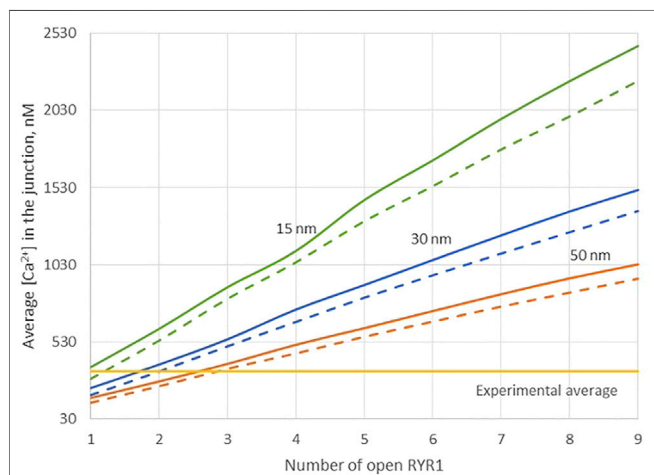


FIGURE 3 | Influence of the value of the distance between the PM and the ERM on the Ca^{2+} microdomains in the ER-PM junction. The green curve (15 nm) corresponds to the situation considered in **Figure 2**. Larger distances, blue curve (30 nm) and orange curve (50 nm) do not influence the low contribution of the opening of the ORAI1 to the Ca^{2+} concentration increase in the junction. Dotted lines represent junctional Ca^{2+} concentration reached in the absence of ORAI1 channels.

express ORAI1, the frequency of occurrence of junctional microdomains is reduced by ~ 10 , while their amplitude is lowered by $\sim 25\%$ (Diercks et al., 2018). We thus concluded that RYR1 located inside the junction, whatever its height, cannot account for experimental observations.

Another possibility would be that RYR1s are located outside the junction, but close to it, in such a way that they affect sub-PM ER Ca^{2+} concentration. Thillaiappan et al. (2017) reported clusters of immobile IP_3Rs surrounding the ER-PM junctions, with the mouths of the IP_3Rs directed towards the PM. In our previous computational study of the IP_3R -dependent, adhesion-induced Ca^{2+} microdomains, we found that simulations based on this configuration agree with experimental observations (Gil et al., 2021). We investigated the possibility that RYR1s are similarly localized around the junction. In this configuration, schematized in **Figure 4**, a ring of RYR1s located in the sub-PM ER membrane and spaced by 90 nm, are releasing Ca^{2+} in the cytosolic space adjacent to the junction. The Ca^{2+} microdomains simulated under this configuration are shown in **Figure 5**, considering 1 (**Figure 5B**, **Supplementary Figure S2**) to 8 (**Figure 5I**) open RYR1. To reach the experimentally observed average amplitude of around 340 nM, seven or eight RYR1 must open simultaneously (**Figure 5J**). This number is slightly affected by the distance between the RYR1 and the junction. If a 45 nm distance is considered, instead of 90 nm as considered in **Figure 5**, opening of five RYR1s simultaneously is sufficient to reach the experimentally observed amplitude in the junction

(**Supplementary Figure S4**). Indeed, a larger amount of the Ca^{2+} released by RYR1 can diffuse into the junction in this configuration. In the absence of ORAI1, the increase in Ca^{2+} in the junction due to RYR1 opening is much below the experimentally observed amplitude of the microdomains. Thus, when the RYR1 located in the membrane of the sub-PM ER are not releasing Ca^{2+} directly in the junctions, the model reproduces the experimental observation that NAADP-induced Ca^{2+} microdomains rely on both RYR1 and ORAI1 (Diercks et al., 2018).

Observations in T cells indicate that Ca^{2+} signals in the junction are rather stereotypic, with a relatively constant amplitude (Diercks et al., 2018). It is thus expected that the microdomain characteristics are not very sensitive to the numbers of RYR1 present around the junction. We next investigated the influence of the number of open RYR1 in more detail, considering the possibility that up to 16 RYR1 are located around the junction. This was done in the simulations by considering another ring of eight receptors 90 nm below the first one. As visible in **Figure 6A**, the relation between the amplitude of the simulated microdomains and the number of open RYR1 is non-linear with a marked stepwise behaviour. From one to three open RYR1, the increase in amplitude is linear. All five STIM1/2 bound ORAI1 channels are in their lowest conductance state (**Figure 6B**) and the Ca^{2+} increase in the junction is due to diffusion from the adjacent cytosol. From four open RYR1 on, local ER Ca^{2+} depletion is sufficient to further activate ORAI1 creating changes in the slope of the relation between the amplitude of the Ca^{2+} signal and the number of open receptors. If more than eight RYR1 open simultaneously, additional ones do not activate ORAI1 further. As seen in **Supplementary Figure S1**, the 54% opening state is reached when the value of C_S in the close vicinity of STIM1/2 bound to ORAI1 reaches 260 μM . This would require a Ca^{2+} decrease at the ER lumen close to RYR1 channel that is not reached under localised Ca^{2+} signaling because of fast diffusion-mediated replenishment. From 8 to 16 open RYR1, local depletion is not much affected, with a minimal ER Ca^{2+} concentration that remains around 340 μM as visible in **Figure 7** that shows a cross-sectional view of the Ca^{2+} concentrations in the sub-PM ER and in the cytoplasmic space including the junction (see also **Supplementary Figure S3** for cross-sections). Noticeably, Ca^{2+} concentrations at the cytosolic side of RYR1 slightly decrease with the number of open receptors, from 17.5 to 15.9 μM for 2 and 16 open receptors, respectively. The slight decrease in the Ca^{2+} gradient at the channel pore indeed reduces the flux through the RYR1. Thus, increasing the number of RYR1 leads to a decrease in the ER Ca^{2+} concentration around STIM1/2, but this decrease is not sufficient to provoke the passage of ORAI1 channels to a higher conductance state.

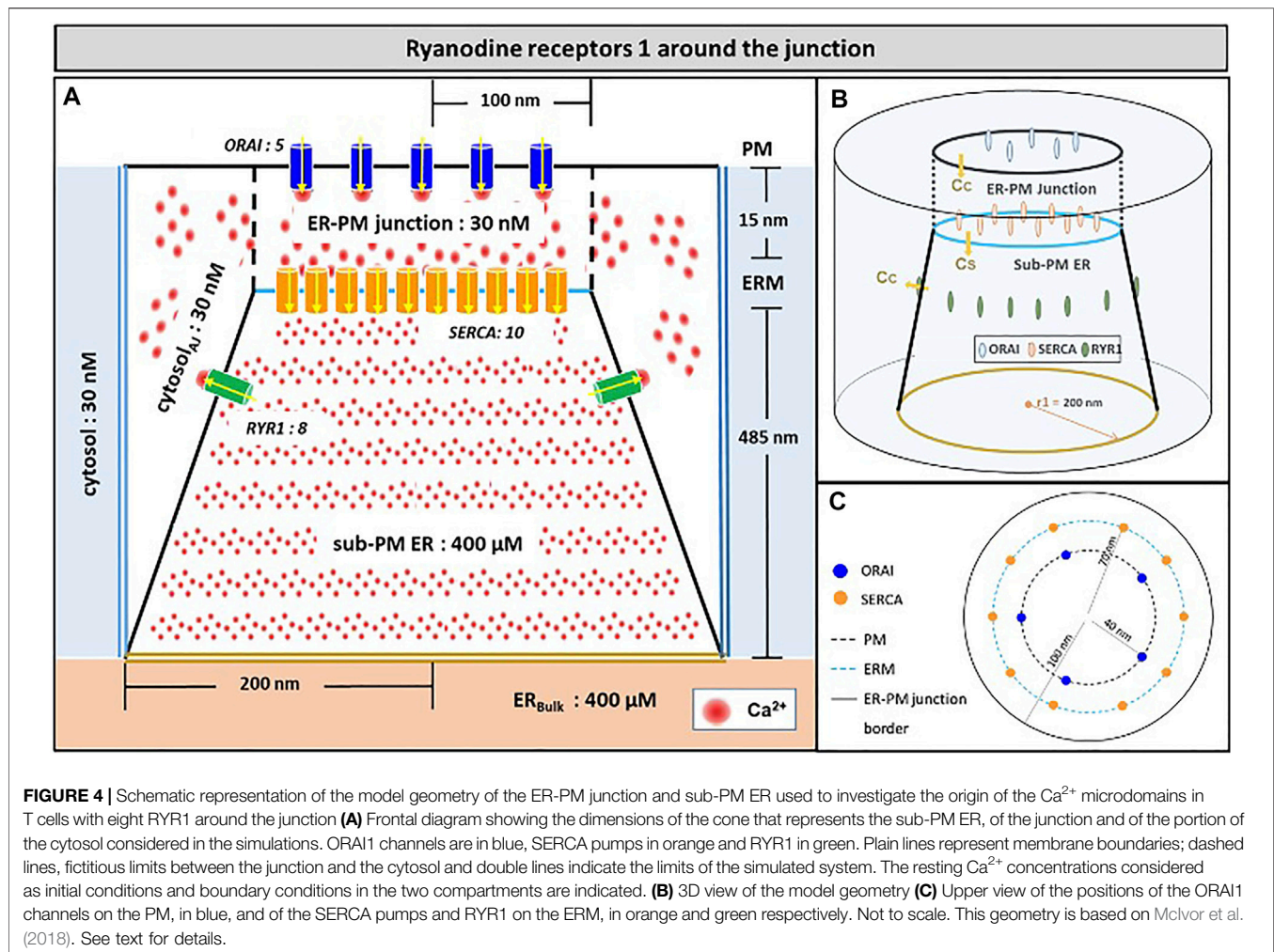


FIGURE 4 | Schematic representation of the model geometry of the ER-PM junction and sub-PM ER used to investigate the origin of the Ca^{2+} microdomains in T cells with eight RYR1 around the junction **(A)** Frontal diagram showing the dimensions of the cone that represents the sub-PM ER, of the junction and of the portion of the cytosol considered in the simulations. ORAI1 channels are in blue, SERCA pumps in orange and RYR1 in green. Plain lines represent membrane boundaries; dashed lines, fictitious limits between the junction and the cytosol and double lines indicate the limits of the simulated system. The resting Ca^{2+} concentrations considered as initial conditions and boundary conditions in the two compartments are indicated. **(B)** 3D view of the model geometry **(C)** Upper view of the positions of the ORAI1 channels on the PM, in blue, and of the SERCA pumps and RYR1 on the ERM, in orange and green respectively. Not to scale. This geometry is based on McIvor et al. (2018). See text for details.

NAADP-induced Ca^{2+} microdomains observed early after T cell stimulation thus rely on the simultaneous opening of an average of seven–eight RYR1 located around the ER-PM junction.

Predicted Type 1 Ryanodine Receptors Involvement in the Formation of Microdomains Agree With Type 1 Ryanodine Receptors Open Probabilities in the Presence of NAADP

Simulation results obtained in the previous section indicate that best agreement between modelled and experimentally observed microdomains occur when most of the eight RYR1 located near the preformed ORAI1/STIM1/STIM2 complexes are open simultaneously during 64 ms. This conclusion stems from a direct comparison between the simulated and experimentally observed Ca^{2+} signals. To further validate this result, some reasoning based on RYR1 open probability can be proposed. The 64 ms duration of a Ca^{2+} microdomain corresponds to the average duration of the NAADP-evoked Ca^{2+} signals arising in the first 15 s after TCR activation (Diercks et al., 2018).

Interestingly, 64 ms also fits in the range of the reported durations of Ca^{2+} sparks (Jaggard et al., 2000). It is thus likely that in response to the TCR/CD3 stimulation-induced NAADP increase, RYR1 undergo repetitive openings maintained by Ca^{2+} -induced Ca^{2+} -release, a process that generates a small amplitude Ca^{2+} increase in the cytosol, called “spark”. The decrease of ER Ca^{2+} that accompanies the spark is in turn responsible for the opening of ORAI1, and thus for the Ca^{2+} microdomain in the junction.

We thus investigated if our conclusions about the molecular mechanism underlying TCR/CD3-induced Ca^{2+} microdomains are compatible with the dynamics of RYR1 during spark-like activity. Upon TCR/CD3 stimulation, global NAADP concentration in T cells increases from $4.1 \pm 1.5 \text{ nM}$ to $33.6 \pm 7.2 \text{ nM}$ (Gasser et al., 2006). Because RYR1 are activated by NAADP in T cells (Wolf et al., 2015; Diercks et al., 2018; Roggenkamp et al., 2021), their Ca^{2+} -releasing activity will increase. Indeed, Hohenegger et al. (2002) have shown that the open probability of these receptors is a highly nonlinear function of NAADP concentration, with an EC_{50} of $31.2 \pm 6.9 \text{ nM}$. Because NAADP synthesis occurs near the ER-PM junctions (Gu

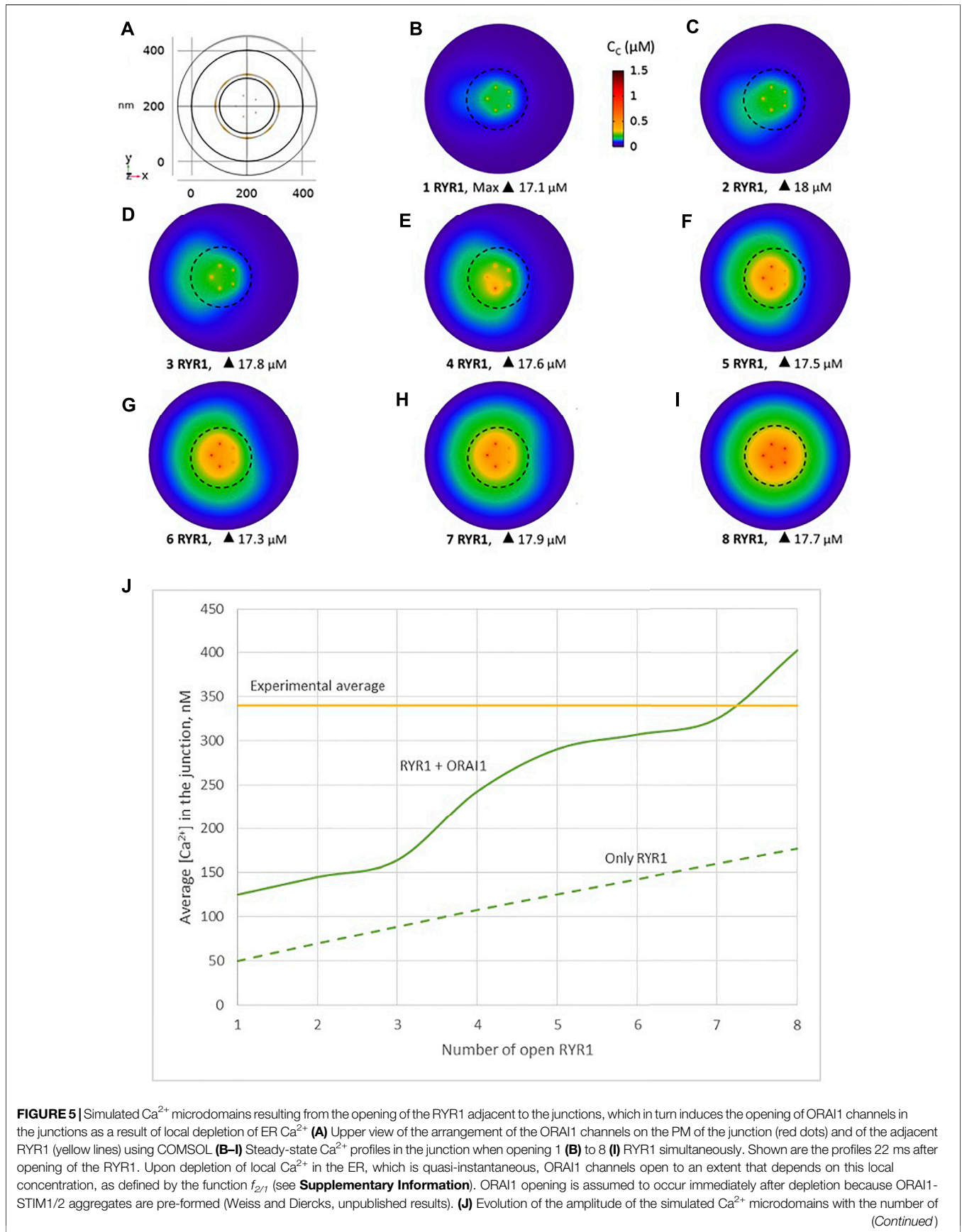
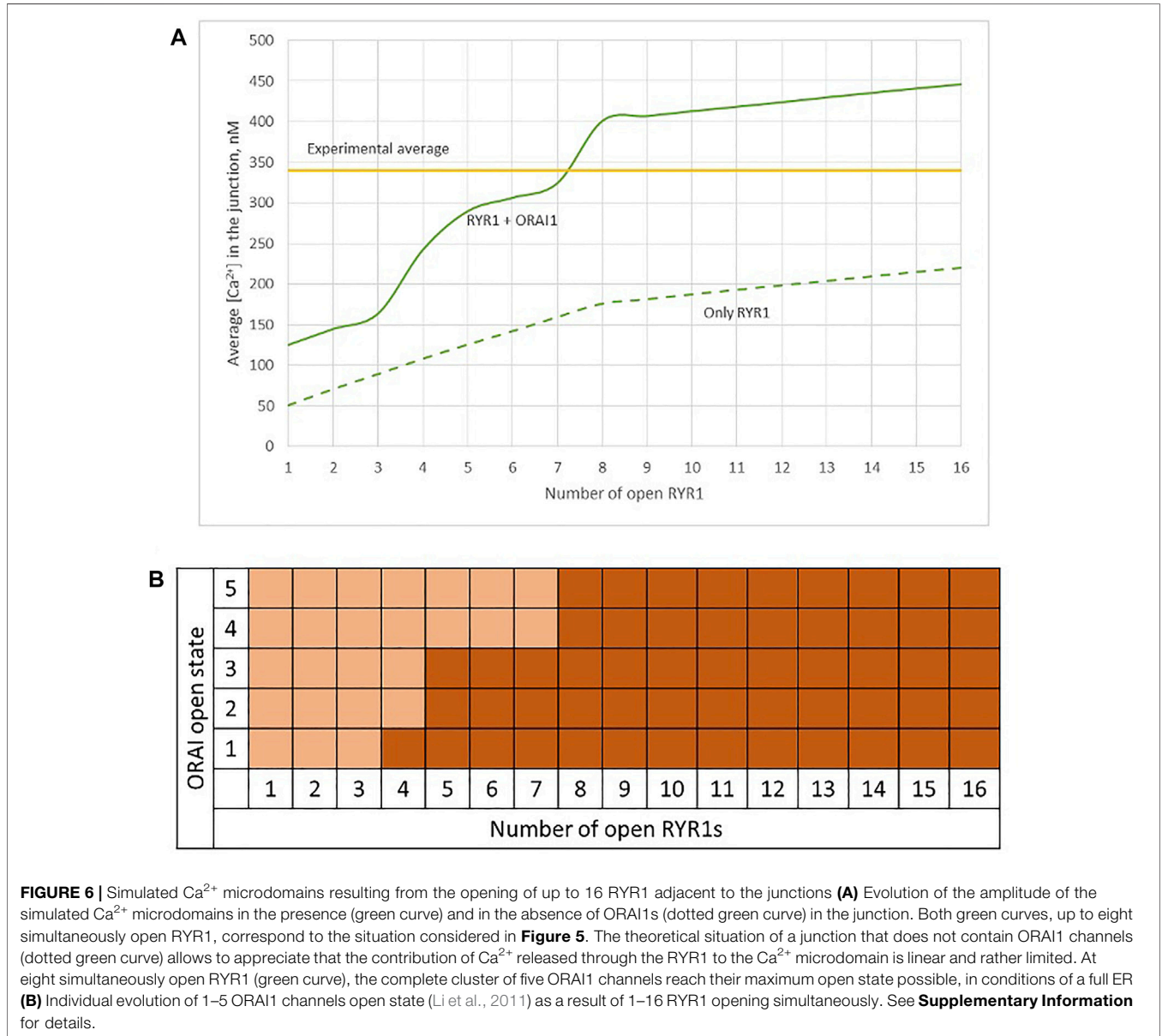


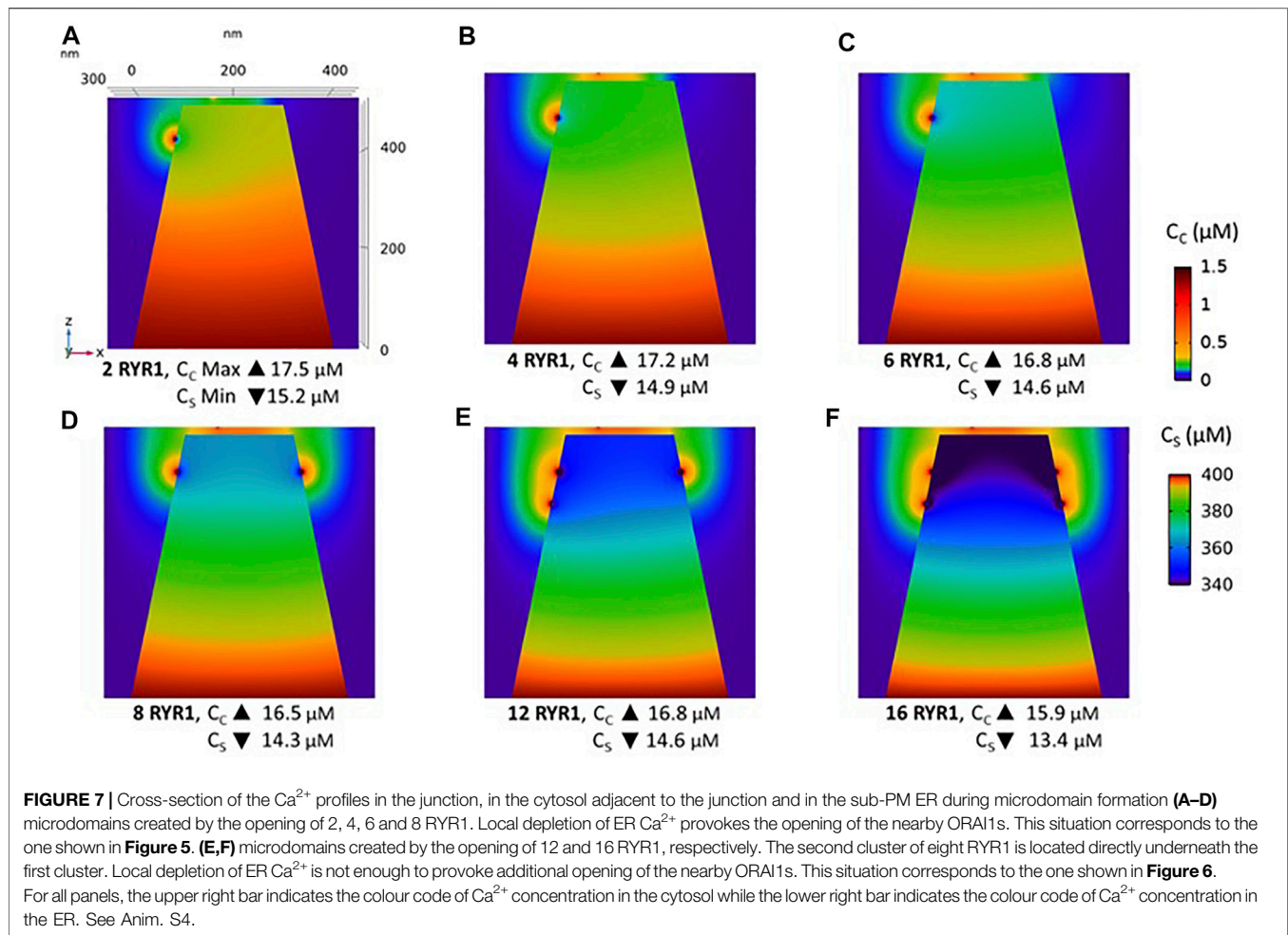
FIGURE 5 | Simulated Ca^{2+} microdomains resulting from the opening of the RYR1 adjacent to the junctions, which in turn induces the opening of ORAI1 channels in the junctions as a result of local depletion of ER Ca^{2+} (A) Upper view of the arrangement of the ORAI1 channels on the PM of the junction (red dots) and of the adjacent RYR1 (yellow lines) using COMSOL (B–I) Steady-state Ca^{2+} profiles in the junction when opening 1 (B) to 8 (I) RYR1 simultaneously. Shown are the profiles 22 ms after opening of the RYR1. Upon depletion of local Ca^{2+} in the ER, which is quasi-instantaneous, ORAI1 channels open to an extent that depends on this local concentration, as defined by the function $f_{2/1}$ (see **Supplementary Information**). ORAI1 opening is assumed to occur immediately after depletion because ORAI1-STIM1/2 aggregates are pre-formed (Weiss and Diercks, unpublished results). (J) Evolution of the amplitude of the simulated Ca^{2+} microdomains with the number of (Continued)

FIGURE 5 | simultaneously open RYR1 in the junction, showing that experimentally observed microdomains can in principle result from the opening of ORAI1 channels induced by the spontaneous opening of a few RYR1 near the junction, in conditions of a full ER. Dotted line represents junctional Ca²⁺ concentration reached in the absence of ORAI1 channels. See Anim. S2a,b,c,d and S3 in **Supplementary Information**.



et al., 2021), local concentrations in the vicinity of RYR1 are certainly larger than the average values mentioned above and likely exceed the EC₅₀. Thus, the open probability of RYR1 near the junctions must be of the order of 0.7, which is the maximal value measured at 20 μM Ca²⁺. Given that the mean open time of RYR1 is ~2 ms (des Georges et al., 2016; Sato & Bers, 2011), the mean closed time in these conditions can be estimated to be 0.86 ms. On the basis of these data, one can obtain a rough approximation of the number of simultaneously open receptors in a spark site when RYR1s

are maximally activated by NAADP. Straightforward stochastic simulations of opening and closing of eight RYR1 with average opening and closing times equal to 2 and 0.86 ms, respectively, indicate that most of the time, six receptors are simultaneously open (**Figure 8A**). This result was obtained by performing 64 ms long stochastic simulations of eight independent RYR1 and determining at each time step how many receptors are open. The maximal frequency at six open receptors is in accordance with the three-dimensional spatio-temporal simulations indicating that best agreement between



experimental observations and computational results is obtained when seven to eight RYR1 are simultaneously open during a 64 ms Ca^{2+} spark, considering the existence of pre-formed STIM1/2 and ORAI1 complexes (**Figure 5**). In contrast, the same calculations predict that for basal NAADP concentrations, when the open probability of RYR1 equals 0.4, the highest frequency corresponds to three RYR1 open simultaneously (**Figure 8B**). In the above simulations (**Figure 5**), this corresponds to a Ca^{2+} microdomain with an amplitude well below the experimental average. Similar stochastic simulations (**Supplementary Figure S5** and related text in the SI) indicate that for the IP_3 -mediated microdomains corresponding to pre-stimulation conditions, the maximal frequency corresponds to two receptors open simultaneously, in qualitative agreement with our previous results (Gil et al., 2021).

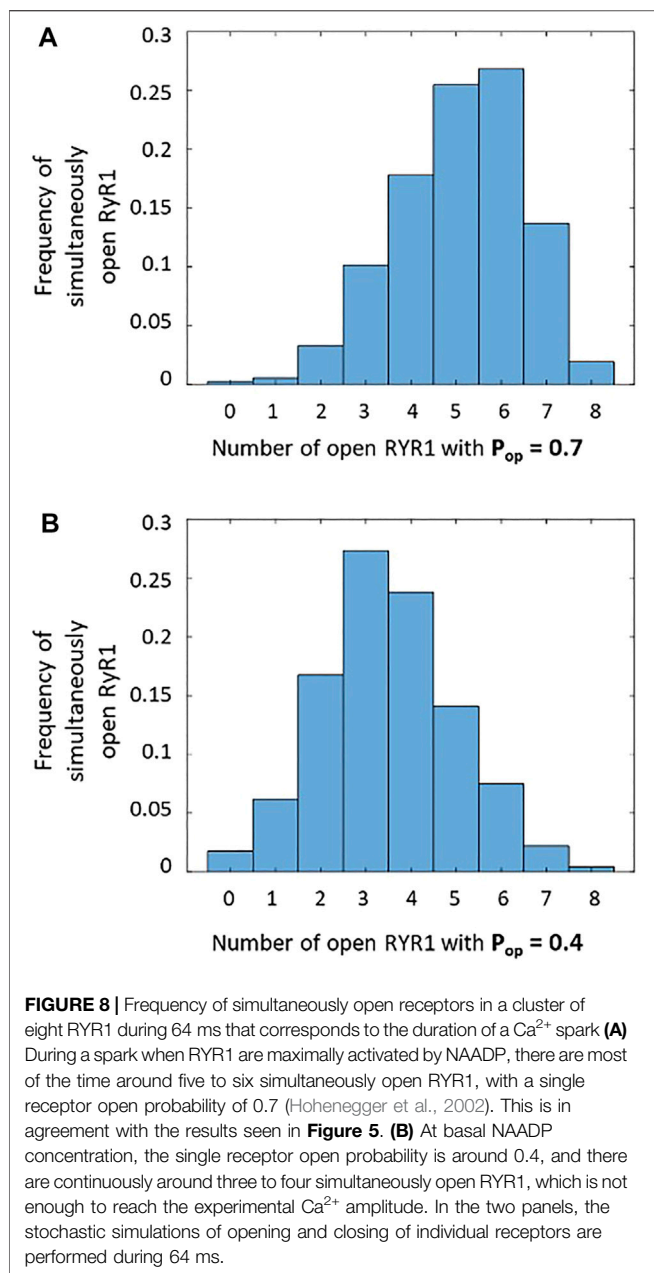
In summary, by combining previous observations about NAADP increase upon TCR/CD3 stimulation of T cells and RYR1 open probability, we conclude that the NAADP-induced increase in the open probability of RYR1 triggers the opening of most of the eight RYR1 located around the ER-PM junction. This is in agreement with the spatio-temporal simulations shown in the previous section, which indicate that Ca^{2+}

microdomains observed early after T cell stimulations rely on the simultaneous opening of seven to eight RYR1 located around the junction.

The Isoforms of STIM That Are Bound to ORAI1 Determine the Characteristics of the Ca^{2+} Microdomains

In the previous sections, we found that the microdomains occurring during the first 15 s after TCR/CD3 stimulation involve a larger number of ER Ca^{2+} releasing channels than those observed before stimulation. Indeed, the local depletion induced by the opening of six–seven RYR1 is needed to activate ORAI1 and reproduce experimentally observed NAADP-dependent microdomains (**Figure 5**) while three to six IP_3 R are involved in the creation of the adhesion-mediated, IP_3 -dependent microdomains (Gil et al., 2021). At first sight, this is paradoxical as the conductance of RYR1 is about 5 times larger than that of IP_3 Rs.

We thus studied the characteristics of the Ca^{2+} increases created by the simultaneous opening of either eight IP_3 Rs or eight RYR1 (see **Table 1**). For the two Ca^{2+} channel types, we considered two possible preformed ORAI1/STIM complexes:



STIM2 homotetramers (STIM2/2) and STIM1 and STIM2 heterotetramers (STIM1/2). Simulation results indicate that the nature of the ER Ca^{2+} release channel does not much influence the characteristics of the Ca^{2+} microdomains. Indeed, the Ca^{2+} signal in the junction is determined by the opening state of ORAI1, which is the same when Ca^{2+} release from the ER is mediated by IP_3Rs or RYR1. The Ca^{2+} concentration sensed by the ORAI1/STIM complex is nearly the same in the two situations. As shown in Figure 9C, once the steady state gradients are established, the fluxes are nearly identical. Because of the slow replenishment around the pore of the receptor channel with $D_s = 10 \mu\text{m}^2/\text{s}$, the concentration gradient around the two extremities of the pore does not

changes drastically and hence the flux remains of the same order for IP_3R and RYR1. In contrast, the nature of the STIM isoforms bound to ORAI1 has a drastic influence on the characteristics of the Ca^{2+} microdomain since it determines their Ca^{2+} sensitivity, and hence the opening state of ORAI1. Because STIM1/2 has a lower sensitivity to ER Ca^{2+} depletion than STIM2/2, the open state of ORAI1 is lower and the increase in Ca^{2+} in the junction has both a smaller amplitude and spatial extent (compare blue to green lines in Figure 9A,B to Figure 6B and Table 1).

Based on these computational observations, the prototypical evolution of Ca^{2+} microdomains from adherent to TCR/CD3 stimulated T cells is proposed to obey the following scenario. Upon adhesion to proteins of the extracellular matrix, integrin evoked IP_3 signaling provokes an increase in the frequency of Ca^{2+} puffs arising from the clusters of IP_3R located near the ER/PM junction. These puffs typically last ~ 44 ms during which, in average, two IP_3Rs are open simultaneously. On the other hand, five ORAI1 channels are located in the PM of the junction and bound to STIM2/2 homotetramers. In response to the decrease in ER Ca^{2+} created by the puff, the ORAI1 channels open to $\sim 21\%$ of their maximal conductance and create the Ca^{2+} microdomain (Figures 10A, 1st row of Table 2). After the Ca^{2+} puff, Ca^{2+} is rapidly replenished in the sub-PM ER and ORAI1 channels shift to their lowest conductance state ($\sim 7\%$ opening) that corresponds to basal Ca^{2+} entry, but not to a detectable Ca^{2+} microdomain (Figure 10B, 2nd row of Table 2) when bound to the STIM1/2 isoform, and stay at 21% when bound to STIM2/2. TCR/CD3 stimulation initiates NAADP signaling, which increases the open probability of the RYR1 located around the junction and thus the frequency of Ca^{2+} sparks (Figure 10C, 3rd row of Table 2). During these events, ~ 6 RYR1 are open simultaneously. At this stage, ORAI1 channels are preferably bound to STIM1/2 heterotetramers, which decreases their sensitivity to ER Ca^{2+} depletion. Thus, as in the case of the IP_3 -dependent microdomains, they open at $\sim 21\%$ of their full capacity. However, because more Ca^{2+} is released in the cytosolic space just around the junction by six RYR1 than by two IP_3R , the Ca^{2+} microdomain in the junction is a bit larger because of diffusion.

DISCUSSION

Activation of T cells is an essential step to start an adaptive immune response. At this particular point a highly important decision is made: whether a T cell stays quiescent or may develop into an effector T cell carrying out immune effector functions to destroy pathogens, or in case of autoimmune reactions, to attack our own body. Among several signaling processes involved, Ca^{2+} signaling is fundamental for T cell activation. In a previous study, we resorted to mathematical modeling to gain insight into the early, small scale Ca^{2+} increases that follow adhesive interactions of T cells, which play a crucial role in T cell migration to inflamed tissue (Weiss

TABLE 1 | Characteristics of the simulated microdomains relying on the simultaneous opening of eight IP₃Rs for 44 ms (first two lines) or of eight RYR1 for 64 ms (lines three and 4). For each case, two situations are considered: the existence of pre-formed clusters of ORAI1 with STIM2/2 homotetramers (lines 1 and 3) and the existence of pre-formed clusters of ORAI1 with STIM2/1 heterotetramers (lines two and 4). Maximal concentrations denote the maximal local concentrations reached in the domains indicated. Spatial extent refers to the area of the junction's portion in which Ca²⁺ concentration exceeds 300 μM. The ER [Ca²⁺] felt by ORAI is the average local concentration of luminal Ca²⁺ around the mouth of the IP₃R or RYR1, computed in a 108 nm³ volume.

| Eight Open Receptors | | Max[Ca ²⁺] in the junction(μM) | Max[Ca ²⁺] around the junction(μM) | Average[Ca ²⁺] in the junction(μM) | Spatial extent (μM ²) | ER[Ca ²⁺] at channel pore(μM) | ER[Ca ²⁺] felt by ORAI(μM) | ORAI mean open state |
|----------------------------|-------------|--|--|--|-----------------------------------|---|--|----------------------|
| IP ₃ R 44 ms | STIM2/ 2 | 10 | 17 | 0.755 | 0.049 | 11 | 331 | 54% |
| | STIM2/ 1 | 354 | 17 | 0.396 | 0.024 | 11 | 331 | 21% |
| RyR 165 ms | STIM2/ 2 | 11 | 18 | 0.762 | 0.049 | 12 | 328 | 54% |
| | STIM2/ 1 | 4.57 | 18 | 0.402 | 0.024 | 12 | 328 | 21% |

and Diercks, unpublished results; Mezu-Ndubuisi & Maheshwari, 2021). Here, we extend this model to investigate the molecular mechanism underlying the early phase of activation following TCR/CD3 stimulation. Although both types of Ca²⁺ microdomains largely rely on Ca²⁺ entry through preformed ORAI1/STIM complexes, the former response relies on IP₃ signaling while the latter involves NAADP and RYRs. Interestingly, a progressive change in STIM isoforms, from mainly STIM2 homotetramers to STIM1/2 heterotetramers, also accompanies this transition (Figure 11). Computational modeling of the spatio-temporal Ca²⁺ dynamics in the ER-PM junctions allowed us to reproduce the observation that the microdomains triggered by cell adhesion or by TCR/CD3 stimulation at its early phase appear rather similar, despite the different underlying mechanisms.

Simulations of the NAADP dependent microdomains quite forwardly predict that RYR1 are most probably located outside the junction, in a region of the ER membrane that is directly adjacent to the junction. This view contrasts with the well-known arrangement of RYR2 in cardiac cells, where they are facing the PM in dyadic clefts (Jones et al., 2018). In principle, a few RYR1 could be located in the ER-PM junction of T cells because the dimensions of its cytoplasmic part (approx. 28 nm × 28 nm × 12 nm, see Lanner et al., 2010) do not exceed the dimensions of the junction. However, Ca²⁺ microdomains simulated with such a spatial arrangement are no longer dependent on ORAI1, since the increase in Ca²⁺ concentration due to the influx mediated by a single RYR into the junction suffices to create a Ca²⁺ signal of the amplitude observed experimentally, which does not agree with experimental results. It is thus most probable that in T cells RYR1 are arranged around the junction, in the same way as IP₃R (Thillaiappan et al., 2017; Taylor and Machaca, 2019).

Computational results indicate that the influx through ORAI1 channels much depends on the STIM isoforms to which it is bound. In the case of local signaling investigated here, the same opening state of ORAI1 is reached after local Ca²⁺ depletion induced by three IP₃R when it is bound to STIM2/2 as after local

Ca²⁺ depletion induced by seven RYR1 when it is bound to STIM1/2. Thus, the change in the nature of the ORAI1/STIM complexes that follow TCR/CD3 stimulation is expected to play a crucial role in maintaining Ca²⁺ signaling localized despite the stimulation of RYR by NAADP. Along this line, Ahmad et al. (2021) have recently shown in HEK293 cells that while clusters of STIM2 represent the sites of SOCE initiation, STIM1 molecules are progressively recruited when cells are exposed to low stimulation.

In contrast, the nature of the ER-releasing Ca²⁺ channel that creates the local depletion in the sub-PM ER, subsequently triggering ORAI1 opening does not have a significant effect. This result is *a priori* surprising given that the RYR1 has a conductance ~5 times larger than the IP₃R. Simulations indicate that the flux is limited by the replenishment of ER Ca²⁺ at the mouth of the channel rather than by its conductance. Thus, the extent of local depletion is imposed by the value of the diffusion coefficient of Ca²⁺ in the ER. This computational observation agrees with the major role played by intraluminal diffusion of Ca²⁺ in setting the responsiveness of Purkinje cells to synaptic inputs (Okubo et al., 2015). It should be kept in mind that the peculiar geometry of the junctional ER is expected to play an important role in decreasing the value of the effective Ca²⁺ diffusion coefficient because of the tortuosity of the tubular network of the ER (Schaff et al., 1997; Oloviczky and Verkman, 1998). In our simulations, diffusion is however fast enough to avoid decreases in local ER Ca²⁺ that would trigger the passage of ORAI1 channels in a highly active state. Simulations indicate that during localized Ca²⁺ signaling in T cells, ORAI1 channels never exceed 21% of their maximal activity.

Together with experimental observations (Diercks et al., 2018; Weiss and Diercks, unpublished results), our computational model ascribes the evolution of Ca²⁺ microdomains from the adherent/pre-stimulated to the TCR/CD3 early stimulated state as a passage from puff-to spark-triggered SOCE. Indeed, while the two types of localized Ca²⁺ signaling rely on ORAI1-mediated Ca²⁺ entry, cell adhesion triggers the synthesis of IP₃, and TCR/CD3

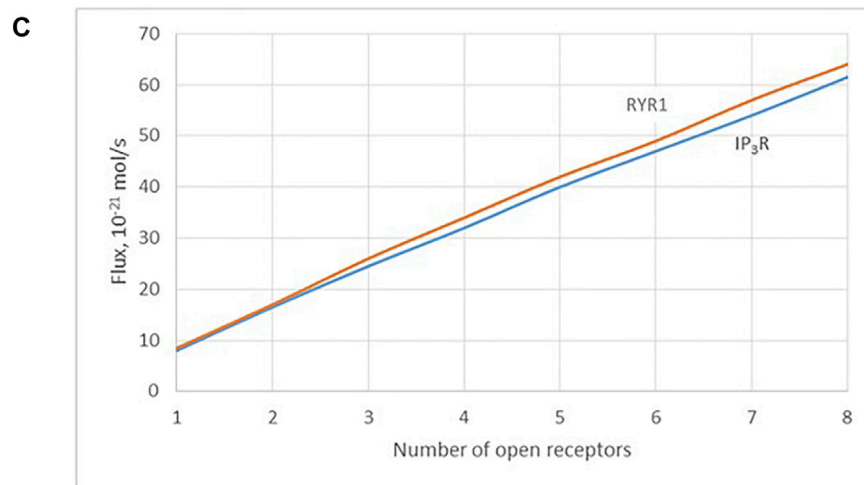
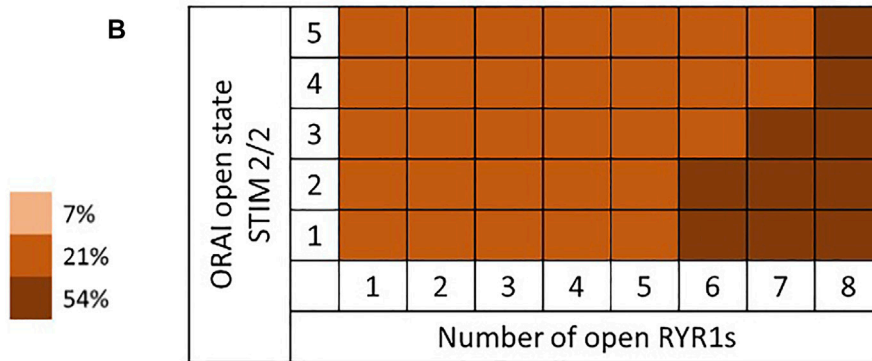
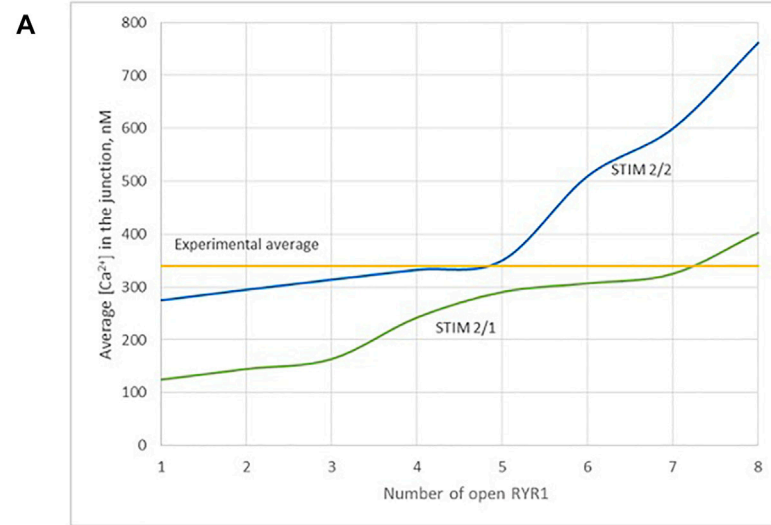


FIGURE 9 | Influence of the nature of the ER Ca²⁺ channel inducing the local depletion of ER Ca²⁺ (IP₃R or RYR1) and of the STIM isoforms bound to ORAI1 on the characteristics of Ca²⁺ microdomains **(A)** Evolution of Ca²⁺ microdomains amplitude with the number of simultaneously open RYR1 in the junction. The microdomains observed in conditions of full ER can be induced by the spontaneous opening of a few RYR1 near the junction that in turn trigger the opening of ORAI1 channels bound to STIM2/2 (blue curve) or to STIM1/2 (green curve). ORAI1 channels open to an extent that depends on local ER Ca²⁺ concentration, as defined by the corresponding function f_2 or $f_{2/1}$ (see **Supplementary Information**) **(B)** Individual evolution between the 5 open states of the ORAI1 (Li et al., 2011), as a result of 1–8 RYR1 opening simultaneously. **(C)** Comparison of Ca²⁺ fluxes through open IP₃Rs and RYR1. Because of the slow replenishment around the pore of the receptor channel with $D_S = 10 \mu\text{m}^2/\text{s}$, the concentration gradient around the two extremities of the pore does not change drastically and hence the flux remains of the same order for IP₃Rs and RYR1.

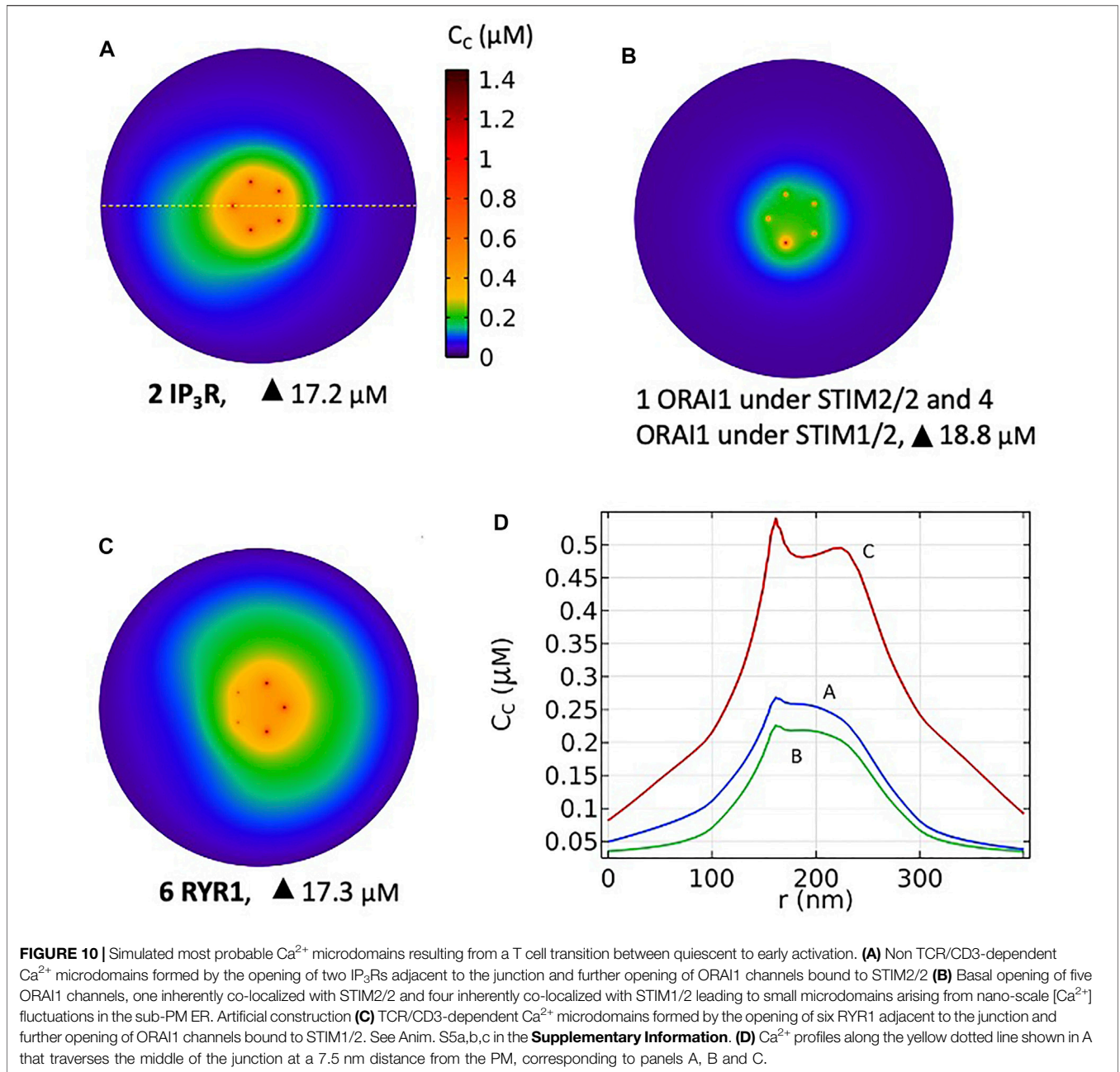


FIGURE 10 | Simulated most probable Ca²⁺ microdomains resulting from a T cell transition between quiescent to early activation. **(A)** Non TCR/CD3-dependent Ca²⁺ microdomains formed by the opening of two IP₃Rs adjacent to the junction and further opening of ORAI1 channels bound to STIM2/2 **(B)** Basal opening of five ORAI1 channels, one inherently co-localized with STIM2/2 and four inherently co-localized with STIM1/2 leading to small microdomains arising from nano-scale [Ca²⁺] fluctuations in the sub-PM ER. Artificial construction **(C)** TCR/CD3-dependent Ca²⁺ microdomains formed by the opening of six RYR1 adjacent to the junction and further opening of ORAI1 channels bound to STIM1/2. See Anim. S5a,b,c in the **Supplementary Information**. **(D)** Ca²⁺ profiles along the yellow dotted line shown in A that traverses the middle of the junction at a 7.5 nm distance from the PM, corresponding to panels A, B and C.

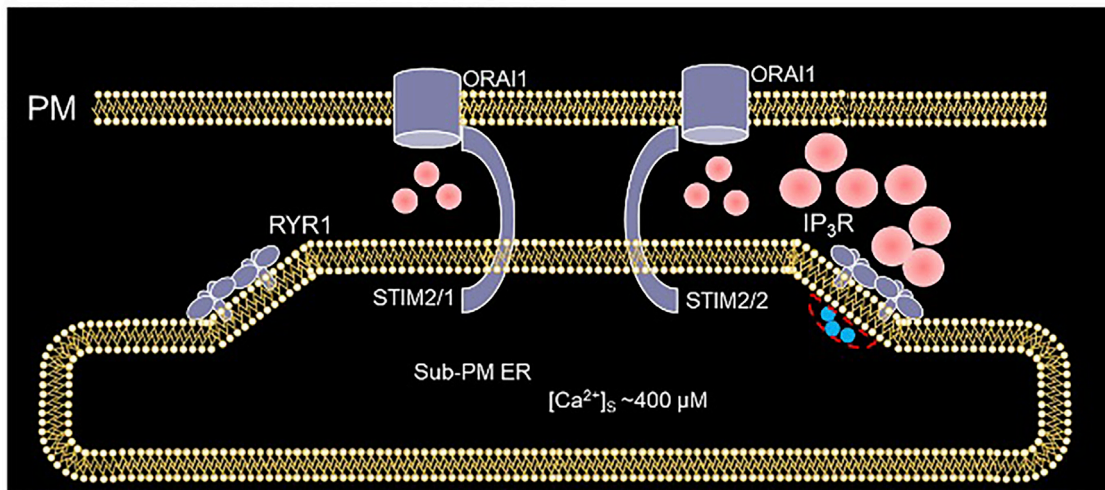
TABLE 2 | Characteristics of the simulated microdomains corresponding to IP₃-dependent Ca²⁺ signaling stimulated by T cell adhesion (line 1), to a spontaneous opening of ORAI in the absence of stimulation (line 2) or to NAADP-dependent Ca²⁺ signaling in response to TCR/CD3 stimulation (line 3)

| — | Average[Ca ²⁺] in the junction(μM) | Spatial extent (μm ²) | ER[Ca ²⁺] felt by ORAI(μM) | ORAI mean open state |
|-----------------------------------|--|-----------------------------------|--|----------------------|
| Puff,2 IP ₃ R; STIM2/2 | 0.293 | 0.0078 | 350 | 21% |
| ORAI,STIM2/2 to STIM2/1 | 0.236 | — | 400 | 7% |
| Spark,6 RYR1; STIM2/1 | 0.307 | 0.0123 | 335 | 21% |

stimulation initially that of NAADP. The respective durations of the two types of Ca²⁺ microdomains (44 ± 4 ms and 64 ± 3 ms) are in the ranges of those reported for puffs (Bootman et al., 1997) and sparks (Jaggard et al., 2000), respectively. In

the two cases, the local depletion in ER Ca²⁺ created by the puff or the spark can trigger ORAI1 opening, with a resulting simulated Ca²⁺ increase in the ER-PM junction that matches experimental observations. Moreover, straightforward

A Adhesion-triggered Ca^{2+} microdomains



B TCR/CD3-triggered Ca^{2+} microdomains

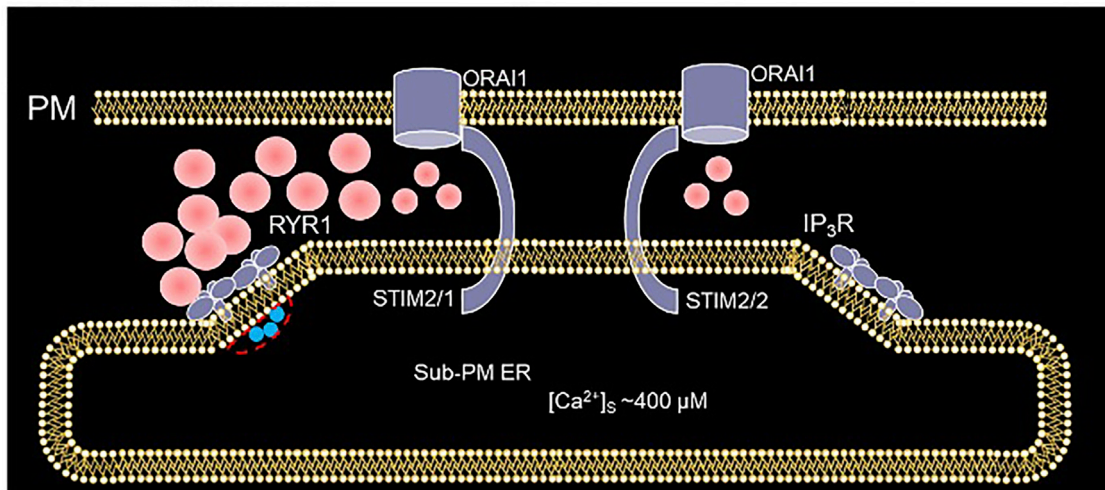


FIGURE 11 | Schematized representation of the proposed mechanism underlying the spontaneous formation of Ca^{2+} microdomains in T cells during its transition from quiescent to early activation **(A)** In an otherwise unstimulated cell, non TCR/CD3 dependent short, spontaneous activation of one or a few IP_3Rs close to the junction, releases Ca^{2+} from the sub-PM ER into the cytosol, leading to further opening of ORAI1 channels most likely bound to STIM2/2 at this stage (Weiss and Diercks, unpublished results) **(B)** During the first 15 s following TCR/CD3 stimulation, and NAADP driven activation of several RYR1 close to the junction, slightly larger amount of Ca^{2+} is released from the sub-PM ER into the cytosol. The resulting local Ca^{2+} depletion close to the RYR1 pore provokes the unbinding of Ca^{2+} from STIM1/2 heterotetramers, which further activates ORAI1 channels (Diercks et al., 2018). Red spots represent Ca^{2+} ions.

stochastic simulations of channel opening and closing taking into account the channels open probabilities in the presence of ligand and high Ca^{2+} concentration indicate a number of simultaneously open receptors matching with the results of the 3D spatiotemporal simulations. In the future, more realistic 3D simulations should be performed to take into account the stochastic nature of puffs and sparks to simulate microdomains, instead of the simplified deterministic description of stereotypic IP_3R - or RYR1-mediated release of ER Ca^{2+} used in the present study.

As another perspective, the present model could be used to investigate how the increase in frequency of RYR1 opening observed ~ 15 s after TCR/CD3 stimulation affects the spatiotemporal dynamics of junctional Ca^{2+} during the transition of T cells towards full activation. In these longer time scales, additional aspects of SOCE regulation should be considered, such as slow Ca^{2+} dependent inactivation (Dagan and Palty, 2021) or the dynamic nature of the ER-PM junctions (Okeke et al., 2016). The extension of the model to several junctions would enable to investigate how

microdomains spread and interact to propagate Ca²⁺ signals deeper into the cell and promote full activation.

DATA AVAILABILITY STATEMENT

The original contributions presented in the study are included in the article/**Supplementary Material**, further inquiries can be directed to the corresponding author.

AUTHOR CONTRIBUTIONS

DG, B-PD, AG and GD contributed to the conceptualization and design of the study. DG, AG and GD contributed to the development and analysis of the model. DG performed all numerical simulations. All authors contributed to the article and approved the submitted version.

REFERENCES

- Ahmad, M., Ong, H. L., Saadi, H., Son, G. Y., Shokatian, Z., Terry, L. E., et al. (2021). Functional Communication between IP₃R and STIM2 at Sub-threshold Stimuli Is a Critical Checkpoint for Initiation of SOCE. *Proc. Natl. Acad. Sci. U S A* 119 (3), e2114928118. doi:10.1073/pnas.2114928118
- Bootman, M., Niggli, E., Berridge, M., and Lipp, P. (1997). Imaging the Hierarchical Ca²⁺ Signalling System in HeLa Cells. *J. Physiol.* 499, 307–314. doi:10.1113/jphysiol.1997.sp021928
- Brandman, O., Liou, J., Park, W. S., and Meyer, T. (2007). STIM2 Is a Feedback Regulator that Stabilizes Basal Cytosolic and Endoplasmic Reticulum Ca²⁺ Levels. *Cell* 131 (7), 1327–1339. doi:10.1016/j.cell.2007.11.039
- Dagan, I., and Palty, R. (2021). Regulation of Store-Operated Ca²⁺ Entry by SARAF. *Cells* 10, 1887. doi:10.3390/cells10081887
- des Georges, A., Clarke, O. B., Zalk, R., Yuan, Q., Condon, K. J., Grassucci, R. A., et al. (2016). Structural Basis for Gating and Activation of RyR1. *Cell* 167 (1), 145–157. doi:10.1016/j.cell.2016.08.075
- Diercks, B. P., Werner, R., Weidemüller, P., Czarniak, F., Hernandez, L., Lehmann, C., et al. (2018). ORAI1, STIM1/2, and RYR1 Shape Subsecond Ca²⁺ Microdomains upon T Cell Activation. *Sci. Signal.* 11 (561), eaat0358. doi:10.1126/scisignal.aat0358
- Feske, S. (2007). Calcium Signalling in Lymphocyte Activation and Disease. *Nat. Rev. Immunol.* 7, 690–702. doi:10.1038/nri2152
- Gasser, A., Bruhn, S., and Guse, A. H. (2006). Second Messenger Function of Nicotinic Acid Adenine Dinucleotide Phosphate Revealed by an Improved Enzymatic Cycling Assay. *J. Biol. Chem.* 281 (25), 16906–16913. doi:10.1074/jbc.m601347200
- Gil, D., Guse, A. H., and Dupont, G. (2021). Three-Dimensional Model of Sub-plasmalemmal Ca²⁺ Microdomains Evoked by the Interplay between ORAI1 and InsP₃ Receptors. *Front. Immunol.* 12, 659790. doi:10.3389/fimmu.2021.659790
- Gu, F., Krüger, A., Roggenkamp, H., Alpers, R., Lodygin, D., Jaquet, V., et al. (2021). DUOX2 Synthesizes NAADP in the Early Phase of T Cell Activation. *Sci. Signaling* 14, eabe3800. doi:10.1126/scisignal.abe3800
- Guo, T., Gillespie, D., and Fill, M. (2012). Ryanodine Receptor Current Amplitude Controls Ca²⁺ Sparks in Cardiac Muscle. *Circ. Res.* 111 (1), 28–36. doi:10.1161/circresaha.112.265652
- Guse, A. H., Gil Montoya, D. C., and Diercks, B.-P. (2021). Mechanisms and Functions of Calcium Microdomains Produced by ORAI Channels, D-Myo-Inositol 1,4,5-trisphosphate Receptors, or Ryanodine Receptors. *Pharmacol. Ther.* 223, 107804. doi:10.1016/j.pharmthera.2021.107804
- Hogan, P. G. (2015). The STIM1-ORAI1 Microdomain. *Cell calcium* 58 (4), 357–367. doi:10.1016/j.ceca.2015.07.001

FUNDING

This work was supported by the Deutsche Forschungsgemeinschaft (DFG) (project number 335447717; SFB1328, project A01 to AG), by the Joachim-Herz-Stiftung (Hamburg), Infectophysics Consortium (project 4; to AG), by NCL-Stiftung Hamburg (to AG), the Hamburg Ministry of Science, Research and Equality (LFF-FV75/0070-134, to AG), and by University Medical Center Hamburg-Eppendorf (M3I consortium, to AG). GD is Research Director at the FNRS.

SUPPLEMENTARY MATERIAL

The Supplementary Material for this article can be found online at: <https://www.frontiersin.org/articles/10.3389/fmolb.2022.811145/full#supplementary-material>

- Hohenegger, M., Suko, J., Gscheidlinger, R., Drobný, H., and Zidar, A. (2002). Nicotinic Acid-Adenine Dinucleotide Phosphate Activates the Skeletal Muscle Ryanodine Receptor. *Biochem. J.* 367 (Pt 2), 423–431. doi:10.1042/BJ20020584
- Jaggard, J. H., Porter, V. A., Lederer, W. J., and Nelson, M. T. (2000). Calcium sparks in Smooth Muscle. *Am. J. Physiology-Cell Physiol.* 278, C235–C256. doi:10.1152/ajpcell.2000.278.2.c235
- Jayasinghe, I., Clowsley, A. H., Lin, R., Lutz, T., Harrison, C., Green, E., et al. (2018). True Molecular Scale Visualization of Variable Clustering Properties of Ryanodine Receptors. *Cel. Rep.* 22 (2), 557–567. doi:10.1016/j.celrep.2017.12.045
- Jones, P. P., MacQuaide, N., and Louch, W. E. (2018). Dyadic Plasticity in Cardiomyocytes. *Front. Physiol.* 9, 1773. doi:10.3389/fphys.2018.01773
- Lanner, J. T., Georgiou, D. K., Joshi, A. D., and Hamilton, S. L. (2010). Ryanodine Receptors: Structure, Expression, Molecular Details, and Function in Calcium Release. *Cold Spring Harbor Perspect. Biol.* 2, a003996. doi:10.1101/cshperspect.a003996
- Lewis, R. S. (2011). Store-operated Calcium Channels: New Perspectives on Mechanism and Function. *Cold Spring Harbor Perspect. Biol.* 3 (12), a003970. doi:10.1101/cshperspect.a003970
- Li, Z., Liu, L., Deng, Y., Ji, W., Du, W., Xu, P., et al. (2011). Graded Activation of CRAC Channel by Binding of Different Numbers of STIM1 to Orail Subunits. *Cell Res* 21 (2), 305–315. doi:10.1038/cr.2010.131
- Luik, R. M., Wang, B., Prakriya, M., Wu, M. M., and Lewis, R. S. (2008). Oligomerization of STIM1 Couples ER Calcium Depletion to CRAC Channel Activation. *Nature* 454 (7203), 538–542. doi:10.1038/nature07065
- Mazel, T., Raymond, R., Raymond-Stintz, M., Jett, S., and Wilson, B. S. (2009). Stochastic Modeling of Calcium in 3D Geometry. *Biophysical J.* 96, 1691–1706. doi:10.1016/j.bpj.2008.10.066
- McIvor, E., Coombes, S., and Thul, R. (2018). Three-dimensional Spatio-Temporal Modelling of Store Operated Ca²⁺ Entry: Insights into ER Refilling and the Spatial Signature of Ca²⁺ Signals. *Cell calcium* 73, 11–24. doi:10.1016/j.ceca.2018.03.006
- Mezu-Ndubuisi, O. J., and Maheshwari, A. (2021). The Role of Integrins in Inflammation and Angiogenesis. *Pediatr. Res.* 89 (7), 1619–1626. doi:10.1038/s41390-020-01177-9
- Okeke, E., Dingsdale, H., Parker, T., Voronina, S., and Tepikin, A. V. (2016). Endoplasmic Reticulum-Plasma Membrane Junctions: Structure, Function and Dynamics. *J. Physiol.* 594, 2837–2847. doi:10.1113/jp271142
- Okubo, Y., Suzuki, J., Kanemaru, K., Nakamura, N., Shibata, T., and Iino, M. (2015). Visualization of Ca²⁺ Filling Mechanisms upon Synaptic Inputs in the Endoplasmic Reticulum of Cerebellar Purkinje Cells. *J. Neurosci.* 35, 15837–15846. doi:10.1523/JNEUROSCI.3487-15.2015
- Oloviczky, B., and Verkman, A. (1998). Monte Carlo Analysis of Obstructed Diffusion in Three Dimensions: Applications to Molecular Diffusion in Organelles. *Biophysical J.* 74, 2722–2730.

- Putney, J. W. (2009). Capacitative Calcium Entry: from Concept to Molecules. *Immunological Rev.* 231 (1), 10–22. doi:10.1111/j.1600-065x.2009.00810.x
- Roggenkamp, H. G., Khansahib, I., Hernandez C. L. C., Zhang, Y., Lodygin, D., Krüger, A., et al. (2021). HN1L/JPT2: A Signaling Protein that Connects NAADP Generation to Ca²⁺ Microdomain Formation. *Sci. signaling* 14 (675), eabd5647. doi:10.1126/scisignal.abd5647
- Rückl, M., and Rüdiger, S. (2016). Calcium Waves in a Grid of Clustered Channels with Synchronous IP₃ Binding and Unbinding. *The Eur. Phys. J. E, Soft matter* 39 (11), 108. doi:10.1140/epje/i2016-16108-4
- Sato, D., and Bers, D. M. (2011). How Does Stochastic Ryanodine Receptor-Mediated Ca Leak Fail to Initiate a Ca Spark. *Biophysical J.* 101 (10), 2370–2379. doi:10.1016/j.bpj.2011.10.017
- Schaff, J., Fink, C. C., Slepchenko, B., Carson, J. H., and Loew, L. M. (1997). A General Computational Framework for Modeling Cellular Structure and Function. *Biophysical J.* 73, 1135–1146. doi:10.1016/s0006-3495(97)78146-3
- Solovey, G., Fraiman, D., Pando, B., and Ponce Dawson, S. (2008). Simplified Model of Cytosolic Ca²⁺ Dynamics in the Presence of One or Several Clusters of Ca²⁺-release Channels. *Phys. Rev. E Stat. Nonlin Soft Matter Phys.* 78 (4 Pt 1), 041915. doi:10.1103/PhysRevE.78.041915
- Stathopoulos, P. B., Li, G.-Y., Plevin, M. J., Ames, J. B., and Ikura, M. (2006). Stored Ca²⁺ Depletion-Induced Oligomerization of Stromal Interaction Molecule 1 (STIM1) via the EF-SAM Region. *J. Biol. Chem.* 281 (47), 35855–35862. doi:10.1074/jbc.m608247200
- Streb, H., Irvine, R. F., Berridge, M. J., and Schulz, I. (1983). Release of Ca²⁺ from a Nonmitochondrial Intracellular Store in Pancreatic Acinar Cells by Inositol-1,4,5-Trisphosphate. *Nature* 306 (5938), 67–69. doi:10.1038/306067a0
- Swaminathan, D., Ullah, G., and Jung, P. (2009). A Simple Sequential-Binding Model for Calcium Puffs. *Chaos* 19 (3), 037109. doi:10.1063/1.3152227
- Taylor, C. W., and Machaca, K. (2019). IP₃ Receptors and Store-Operated Ca²⁺ Entry: a License to Fill. *Curr. Opin. Cell Biol.* 57, 1–7. doi:10.1016/jceb.2018.10.001
- Thillaiappan, N. B., Chavda, A. P., Tovey, S. C., Prole, D. L., and Taylor, C. W. (2017). Ca²⁺ Signals Initiate at Immobile IP₃ Receptors Adjacent to ER-Plasma Membrane Junctions. *Nat. Commun.* 8 (1), 1505. doi:10.1038/s41467-017-01644-8
- Thul, R., Thurley, K., and Falcke, M. (2009). Toward a Predictive Model of Ca²⁺ Puffs. *Chaos* 19 (3), 037108. doi:10.1063/1.3183809
- Trebak, M., and Kinet, J.-P. (2019). Calcium Signalling in T Cells. *Nat. Rev. Immunol.* 19 (3), 154–169. doi:10.1038/s41577-018-0110-7
- Walker, M. A., Gurev, V., Rice, J. J., Greenstein, J. L., and Winslow, R. L. (2017). Estimating the Probabilities of Rare Arrhythmic Events in Multiscale Computational Models of Cardiac Cells and Tissue. *Plos Comput. Biol.* 13 (11), e1005783. doi:10.1371/journal.pcbi.1005783
- Wolf, I. M., Diercks, B. P., Gattkowsky, E., Czarniak, F., Kempinski, J., Werner, R., et al. (2015). Frontrunners of T Cell Activation: Initial, Localized Ca²⁺ Signals Mediated by NAADP and the Type 1 Ryanodine Receptor. *Sci. Signal.* 8 (398), ra102. doi:10.1126/scisignal.aab0863
- Wu, M. M., Buchanan, J., Luik, R. M., and Lewis, R. S. (2006). Ca²⁺ Store Depletion Causes STIM1 to Accumulate in ER Regions Closely Associated with the Plasma Membrane. *J. Cell Biol.* 174 (6), 803–813. doi:10.1083/jcb.200604014
- Yin, C.-C., D'Cruz, L. G., and Lai, F. A. (2008). Ryanodine Receptor Arrays: Not Just a Pretty Pattern. *Trends Cell Biology* 18 (4), 149–156. doi:10.1016/j.tcb.2008.02.003

Conflict of Interest: The authors declare that the research was conducted in the absence of any commercial or financial relationships that could be construed as a potential conflict of interest.

Publisher's Note: All claims expressed in this article are solely those of the authors and do not necessarily represent those of their affiliated organizations, or those of the publisher, the editors and the reviewers. Any product that may be evaluated in this article, or claim that may be made by its manufacturer, is not guaranteed or endorsed by the publisher.

Copyright © 2022 Gil, Diercks, Guse and Dupont. This is an open-access article distributed under the terms of the Creative Commons Attribution License (CC BY). The use, distribution or reproduction in other forums is permitted, provided the original author(s) and the copyright owner(s) are credited and that the original publication in this journal is cited, in accordance with accepted academic practice. No use, distribution or reproduction is permitted which does not comply with these terms.